Inorganic Chemistry

Article

pubs.acs.org/IC

Trans Effect in Halobismuthates and Haloantimonates Revisited. Molecular Structures and Vibrations from Theoretical Calculations

Hong-Li Sheu and Jaan Laane*

Department of Chemistry, Texas A&M University, College Station, Texas 77843-3255, United States

Supporting Information

ABSTRACT: Ab initio and density functional theory computations have been carried out to calculate the structures and vibrational spectra of halobismuthates and haloantimonates of formulas $MX6^{3-}$, $M_2X_{10}^{4-}$, and $M_2X_9^{3-}$ for M = Bi or Sb and X = I, Br, or Cl. The results have been compared to experimental crystal structures and the infrared and Raman spectra of these species as well as the $(MX_5^{2-})_n$ and $(MX_4^{1-})_n$ anions. Even though the calculations neglect the effect of which cation is present, they do a good job in verifying the observed trends in bond distances and bond stretching vibrational frequencies. External bonds across from bridging bonds are the shortest and have the highest stretching frequencies for all of the ions investigated. This supports the previously postulated "*trans* effect". Since the calculations were carried out for individual noninteracting anions, the computed results can be expected to best represent the idealized species unperturbed by the effect of the cations present. The *trans* effect results in shortening of the M−X bonds by 0.08−0.13 Å. It also leads to frequency increases of about 20% for the M−X stretching vibrations.

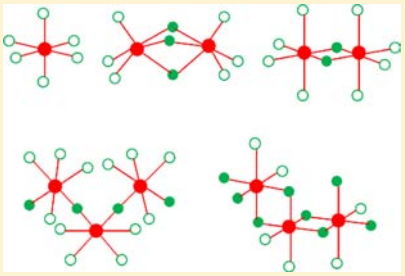

INTRODUCTION

The halobismuthate and haloantimonate anions possess a variety of interesting structures which possess both external and bridging M−X bonds (X = I, Br, Cl). The structures of MX_6^{3-}, $M_2X_9^{3-}$, $M_2X_{10}^{4-}$, $(MX_5^{2-})_n$, and $(MX_4^{1-})_n$ anions are shown in Figure 1.

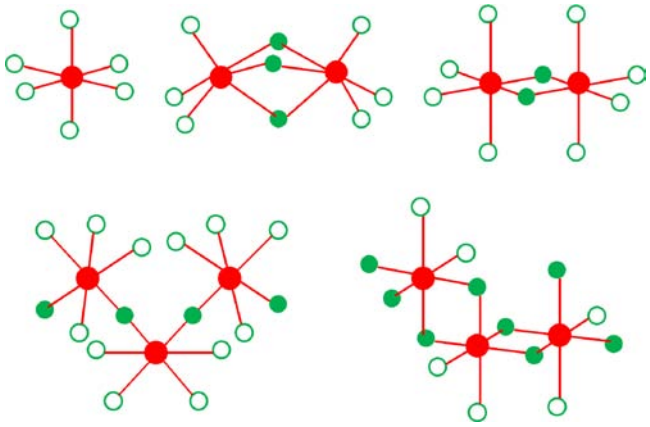

Figure 1. Structures of MX_6^{3-}, $M_2X_9^{3-}$, $M_2X_{10}^{4-}$, $(MX_5^{2-})_n$, and $(MX_4^{1-})_n$ for M = Bi or Sb and X = I, Br, or Cl. The smaller open circles represent external halogen atoms, and the smaller filled circles represent bridging atoms. $(MX_5^{2-})_n$ and $(MX_4^{1-})_n$ are infinite chains.

The latter two have infinite chain structures. In 1980 we reported[1] the far-infrared and low-frequency Raman spectra of several bromo- and iodobismuthates of formulas BiX_6^{3-}, $Bi_2X_9^{3-}$, BiX_5^{2-}, and BiX_4^{1-}. Except for the BiX_6^{3-} species, each of these ions possesses both bridging and nonbridging (external) Bi−X bonds. What we observed was that the Bi−X stretching frequencies for the bridging bonds were the lowest, reflecting the weakest bonds. We also observed that the external Bi−X stretching frequencies for bonds across from Bi−X bridging bonds were higher than those for bonds across from other external Bi−X bonds. We attributed this to a *trans* effect where the weaker bridging bonds across from external Bi−X bonds allow the latter to become stronger. The spectroscopic data were consistent with the crystal structures reported for the iodo and bromo anions[2−22] in that the shortest Bi−X bonds were found when the halogen atom was across from a bridging bond and the longest bonds were found for the bridging bonds.

In 1980 we also reported[23] the low-frequency infrared and Raman data for several bromo- and iodoantimonates. These included SbX_6^{3-}, $Sb_2X_9^{3-}$, SbX_5^{2-}, and SbX_4^{1-} anions associated with several different cations such as *n*-propylammonium and 4-picolinium. As we had observed for the bismuthates, the bridging bonds were the weakest and the strongest external bonds were those *trans* to the bridging bonds. The reported crystal structures[24−33] again showed the same trend as was observed for the bismuthates.

Since the publication of our work described above, a number of crystal structure determinations of chlorobismuthates[34−51] and chloroantimonates[33,52−57] have also been published. In addition, new spectroscopic data have also been reported for the chloro-, bromo-, and iodobismuthates[58−65] and -antimonates.[66−69]

In the present study we have undertaken the calculation of the structures of these anions along with their vibrational frequencies using ab initio (MP2/cc-pVTZ-PP) and density

Received: September 25, 2012
Published: April 1, 2013

   dx.doi.org/10.1021/ic302082a | *Inorg. Chem.* 2013, 52, 4244−4249

functional theory (DFT) (B3LYP/cc-pVTZ-PP) computations. The goal was to confirm and support our previous analysis of the vibrational spectra, which had led us to postulate the *trans* effect. We also wanted to provide an additional perspective to better understand the structural features of these interesting anions, which possess several types of M−X bonds. Moreover, since the computations neglect the effect of neighboring cations, they provide the best representation of the noninteracting anions.

THEORETICAL CALCULATIONS

Figure 1 shows the structures for the MX_6^{3-}, $M_2X_9^{3-}$, and $M_2X_{10}^{4-}$ halobismuthate and haloantimonate anions for which computations were carried out. The MX_6^{3-} cations only have external (nonbridging) halogen atoms, while each of the others have both bridging and external atoms. The $M_2X_{10}^{4-}$ structures had not been observed when we published our previous work,[1,23] but the $Bi_2X_{10}^{4-}$ and $Sb_2X_{10}^{4-}$ anions have now been reported.[15,17−19,41,46−49,56] Our computations for these structures here also provide useful bond distance and vibrational frequency comparisons for the MX_5^{2-} and MX_4^{1-} anions, which actually exist as extended groups of octahedrally surrounded metal atoms joined by bridging M−X−M bonds. The structures of these anions are also shown in Figure 1. Since manageable computations for these infinite chains were not possible, we utilized the $M_2X_{10}^{4-}$ results to also help characterize the different types of M−X bonds in the MX_5^{2-} and MX_4^{1-} anions. The $M_2X_{10}^{4-}$ structure has two M−X−M bridging groups, and each metal atom has two external M−X bonds across from each other and two across (*trans*) from bridging M−X bonds. The external bonds of MX_5^{2-} are of the same type as for our $M_2X_{10}^{4-}$ model, but the halogens of its bridging M−X bonds are bonded to different metal atoms. The actual MX_4^{1-} species have no external bonds *trans* to other external bonds as its external bonds are across from bridging M−X bonds. Each $M_2X_9^{3-}$ anion has six external M−X bonds and three M−X−M bridges.

Computations were carried out by using the Gaussian 09 program.[70] The ab initio calculations were performed using the second-order Moller−Plesset (MP2) calculation method with the cc-pVTZ-PP basis set, and the results were utilized to predict the structures and bond distances of the ions. DFT calculations using the Becke and Lee−Yang−Parr exchange-correlation function (B3LYP) calculation method with the same basis set were used to predict the vibrational frequencies. No frequency scaling was utilized. We have previously utilized similar computations to complement our spectroscopic work on organic and organometallic molecules,[71−75] and other researchers have used the same basis sets for metal-containing molecules such as those with aluminum, gallium, bismuth, antimony, copper, cadmium, silver, gold, vanadium, and rhodium.[76−81]

RESULTS AND DISCUSSION

Table 1 shows the calculated bond distances for the BiX_6^{3-}, $Bi_2X_9^{3-}$, $Bi_2X_{10}^{4-}$, $(BiX_5^{2-})_n$, and $(BiX_4^{1-})_n$ anions for X = I, Br, and Cl. The table also shows the experimental bond distances from a number of crystal structure determinations for different cations. For BiX_6^{3-} anions, the experimental bond distances are somewhat dependent on which cation is present but typically agree within ±0.03 Å for each anion. The computed value is that for a free anion without the presence of the cation. Nonetheless, the agreement between calculated and experimental values is good, with the former values typically about 0.03−0.06 Å larger.

For $Bi_2X_9^{3-}$ anions, two types of Bi−X bonds are present, namely, external bonds across from bridging bonds and bridging bonds across from external bonds. The bridging bonds are calculated to be from 0.15 to 0.22 Å longer than the external bonds. The crystal structure determinations show that the actual bond distances for the bridging bonds are longer by 0.18−0.37 Å. However, the calculations are in quite good agreement when the neglected effect of the cation is considered.

For the $Bi_2X_{10}^{2-}$ and BiX_5^{1-} anions, each ion has two types of external halogen atoms: those across from other external atoms and those across from bridging atoms. Each halobismuthate anion also has bridging atoms across from external atoms. Both calculations and experimental data support the previously postulated *trans* effect.[1] The strongest and shortest bonds are those across from bridging atoms. External bonds across from other external atoms are somewhat longer, while the bridging bonds are the longest. This supports the view that external atoms "fight harder" for electron density than bridging atoms so that the bonds across from them cannot be as strong as those across from bridging atoms. For the $Bi_2Cl_{10}^{4-}$ anions the experimental and calculated distances agree very well for all three types of bonds. For the iodide and bromide ions the calculated external bond distances across from other external atoms agree very well with those from crystal structure determinations, but the external bonds across from bridging atoms are calculated to be slightly higher than observed, while the bridging bond distances are calculated to be a little lower than observed. Table 1 also displays the experimentally determined Bi−X bond distances for the BiX_4^{1-} complexes and compares these to the same types of bonds as in our $Bi_2X_{10}^{4-}$ model. All of the external Bi−X bonds are *trans* to bridging halogens and are therefore among the shortest bonds.

Table 2 presents the data for the SbX_6^{3-}, $Sb_2X_9^{3-}$, $Sb_2X_{10}^{4-}$, $(SbX_5^{2-})_n$, and $(SbX_4^{1-})_n$ anions and shows the calculated and experimental bond distances to be in close agreement. As expected for the SbX_6^{3-} anions, the Sb−X distances are less than those for the corresponding bismuth halides given that antimony is higher in the periodic table than bismuth. The $Sb_2X_9^{3-}$ anions are also similar to the bismuth anions. The bridging bonds are longer than the external bonds, and the calculated values are higher than the experimental values (by 0.07−0.10 Å) for the external bonds but lower (by about 0.10 Å) for the bridging bonds. The difference between computed and experimental bond distances can be attributed to the effect of the cations.

Table 2 also presents the calculations for the $Sb_2X_{10}^{2-}$ anions and compares these to $Sb_2Cl_{10}^{4-}$ and to SbX_5^{1-} experimental data for X = I, Br, and Cl. No crystal structures have been reported for the $Sb_2X_{10}^{2-}$ species for X = I or Br. All of the available data and the calculations again support the concept of the *trans* effect, as the external bonds across from bridging bonds are shorter than those across from other external halogen atoms. The table also displays the experimentally determined Sb−X bond distances for the SbX_4^{1-} complexes and compares these to the same types of bond distances in our $Sb_2X_{10}^{4-}$ model.

Table 3 summarizes the bond distance data for the bismuthates and antimonates and clearly displays the magnitude of the *trans* effect. In all cases the shortest bonds are for the external M−X bonds across from the bridging halogen atoms. For the bismuthates the external Bi−X bonds across from other external bonds are calculated to be 0.085−0.110 Å longer than those across from bridging bonds. From crystal structure determinations these are 0.082−0.131 Å longer. The difference arises from the fact that the calculations correspond to values for the free ions not interacting with the neighboring cations. The external Sb−X bonds across from other external atoms are calculated to be longer by 0.095 Å for Sb−I bonds, by 0.104 Å for Sb−Br bonds, and by 0.156 Å for Sb−Cl bonds than those across from bridging bonds. From the crystal structure determinations, the same Sb−Br bonds are 0.179 Å longer and the Sb−Cl bonds are 0.265 Å longer.

In addition to calculating the bond distances for the bismuth and antimony ions, we have also calculated their vibrational

dx.doi.org/10.1021/ic302082a | Inorg. Chem. 2013, 52, 4244−4249

Table 1. Observed and Calculated Bond Distances (Å) of BiX_6^{3-}, $Bi_2X_9^{3-}$, $Bi_2X_{10}^{4-}$, BiX_5^{2-}, and BiX^{4-} Complexes

anion	type	*trans*-halogen	calcd	obsd	ref
BiI_6^{3-}	external	external	3.119	3.087	2
				3.065	3
				3.092	4
$BiBr_6^{3-}$	external	external	2.905	2.853	5
				2.857	6
				2.843	7
				2.840	8
$BiCl_6^{3-}$	external	external	2.770	2.731	34
				2.738	35
				2.703	36
				2.717	37
				2.710	38
				2.705	39
				2.719	40
				2.702	41
				2.660	42
				2.715	43
$Bi_2I_9^{3-}$	external	bridging	3.005	2.920	9
				2.976	10
				2.973	11
	bridging	external	3.159	3.244	9
				3.228	10
				3.227	11
$Bi_2Br_9^{3-}$	external	bridging	2.781	2.713	12
				2.749	13
				2.713	14
	bridging	external	2.972	3.036	12
				3.050	13
				2.979	14
$Bi_2Cl_9^{3-}$	external	bridging	2.635	2.590	44
				2.558	45
$Bi_2Cl_9^{3-}$	bridging	external	2.858	2.827	44
				2.926	45
$Bi_2I_{10}^{4-}$	external	bridging	2.987	2.933	15
	external	external	3.046	3.083	15
	bridging	external	3.130	3.258	15
BiI_5^{2-}	external	bridging	2.987[a]	2.949	16
	external	external	3.046[a]	3.069	16
	bridging	external	3.130[a]	3.278	16
$Bi_2Br_{10}^{4-}$	external	bridging	2.788	2.730	17
				2.730	18
				2.786	19
	external	external	2.835	2.837	17
				2.850	18
				2.808	19
	bridging	external	2.979	3.050	17
				3.060	18
				3.021	19
$BiBr_5^{2-}$	external	bridging	2.788[a]	2.684	20
	external	external	2.835[a]	2.851	20
	bridging	external	2.979[a]	3.071	20
$Bi_2Cl_{10}^{4-}$	external	bridging	2.608	2.607	46
				2.601	47
				2.580	48
				2.568	41
				2.556	49
$Bi_2Cl_{10}^{4-}$	external	external	2.693	2.686	46
				2.712	47
				2.700	48
				2.667	41
				2.697	49
	bridging	external	2.887	2.862	46
				2.855	47
				2.725	48
				2.970	41
				2.915	49
$BiCl_5^{2-}$	external	bridging	2.608[a]	2.546	50
	external	external	2.693[a]	2.696	50
	bridging	external	2.887[a]	2.836	50
BiI_4^{1-}	external	bridging	2.987[a]	2.930	21
	bridging	external	3.130[a]	3.203	21
$BiBr_4^{1-}$	external	bridging	2.788[a]	2.640	22
	bridging	external	2.979[a]	3.038	22
$BiCl_4^{1-}$	external	bridging	2.608[a]	2.526	51
	bridging	external	2.887[a]	2.841	51

[a]Calculated values are from the $Bi_2X_{10}^{4-}$ computations.

frequencies using DFT computations. The crystalline materials have well-defined bond stretching frequencies,[1,23] but the low-frequency bending modes and lattice modes are difficult to distinguish from each other. Hence, since the computations do not take into account any intermolecular or interionic interactions, we focused on comparing only the calculated frequencies for the stretching modes to the experimental ones since these are least affected by the interactions. In the main text of the paper we present only a summary of the vibrational results. The specific details for the individual anions are available in the Supporting Information.

In our previous work[1,23] we analyzed the experimental far-infrared and low-frequency Raman spectra of these anions in detail and assigned the spectra on the basis of octahedral symmetry for the MX_6^{3-} species, C_{2v} for MX_5^{2-}, C_{2v} for MX_4^{1-}, and D_{3h} for $M_2X_9^{3-}$. Each of these has several M−X stretching modes which extend over a range of frequencies. These can be classified as υ_{EE}, where the external M−X bond stretches across from another external bond, as υ_{EB}, where the external bond stretches across from a bridging bond, or as υ_B, for the stretching of a bridging bond. There are also a number of bending vibrations which are of lower frequency. The bending modes interact extensively with the lattice modes of the crystalline structures, and therefore, the computation of these frequencies is not particularly meaningful. They also couple somewhat with the stretching modes as shown from our potential energy distribution (PED) calculations (see the Supporting Information). Our calculations for the molecular vibrations were carried out for independent "gas-phase" species, which have no interactions with the cations or the lattice modes of the solid. Hence, we concentrated on comparing the calculated M−X stretching frequencies to those experimentally observed. In the Supporting Information we present the details of the vibrational calculations and compare the results to previous experimental data. Many of the previous spectroscopic results come from our previous work,[1,23] but infrared and Raman data from other laboratories are also included. The quality of some of the latter is variable. Because there is a very large amount of data for the 19 different halobismuthates and haloantimonates which we investigated, it is not included in the main text. Tables S1−S3

dx.doi.org/10.1021/ic302082a | Inorg. Chem. 2013, 52, 4244−4249

Table 2. Observed and Calculated Bond Distances (Å) of SbX_6^{3-}, $Sb_2X_9^{3-}$, $Sb_2X_{10}^{4-}$, SbX_5^{2-}, and SbX_4^{1-} Complexes

anion	type	*trans*-halogen	calcd	obsd	ref
SbI_6^{3-}	external	external	3.068	N/A	
$SbBr_6^{3-}$	external	external	2.857	2.826	24
				2.809	25
$SbCl_6^{3-}$	external	external	2.720	2.705	52
				2.675	53
				2.643	54
$Sb_2I_9^{3-}$	external	bridging	2.950	2.881	26
				2.870	27
				2.862	28
	bridging	external	3.105	3.252	26
				3.198	27
				3.199	28
$Sb_2Br_9^{3-}$	external	bridging	2.717	2.639	12
				2.630	29
				2.625	30
	bridging	external	2.939	3.034	12
				3.072	29
				3.043	30
$Sb_2Cl_9^{3-}$	external	bridging	2.557	2.455	55
	bridging	external	2.848	2.911	55
$Sb_2I_{10}^{4-}$	external	bridging	2.921	N/A	
	external	external	2.994	N/A	
	bridging	external	3.091	N/A	
SbI_5^{1-}	external	bridging	2.921[a]	2.876	31
	external	external	2.994[a]	3.012	31
	bridging	external	3.091[a]	3.190	31
$Sb_2Br_{10}^{4-}$	external	bridging	2.717	N/A	
	external	external	2.785	N/A	
	bridging	external	2.960	N/A	
$SbBr_5^{1-}$	external	bridging	2.717[a]	2.681	32
	external	external	2.785[a]	2.796	32
	bridging	external	2.960[a]	3.014	32
$Sb_2Cl_{10}^{4-}$	external	bridging	2.482	2.396	56
	external	external	2.631	2.650	56
	bridging	external	2.981	3.013	56
$SbCl_5^{1-}$	external	bridging	2.482[a]	2.452	57
	external	external	2.631[a]	2.734	57
	bridging	external	2.981[a]	2.916	57
SbI_4	external	bridging	2.921[a]	N/A	
	bridging	external	3.091[a]	N/A	
$SbBr_4^{1-}$	external	bridging	2.717[a]	2.567	33
	bridging	external	2.960[a]	2.816	33
$SbCl_4^{1-}$	external	bridging	2.482[a]	2.394	33
	bridging	external	2.981[a]	2.659	33

[a]Calculated values are from the $Sb_2X_{10}^{4-}$ computations.

Table 3. Average M−X Bond Distances (Å) for Different Types of Bonds

			average bond distance	
M−X	type	*trans*-halogen	calcd	obsd
Bi−I	external	bridging	2.996 ± 0.009	2.951 ± 0.031
	external	external	3.083 ± 0.037	3.082 ± 0.017
	bridging	external	3.145 ± 0.015	3.239 ± 0.039
Bi−Br	external	bridging	2.785 ± 0.004	2.759 ± 0.046
	external	external	2.870 ± 0.035	2.841 ± 0.033
	bridging	external	2.976 ± 0.004	3.043 ± 0.064
Bi−Cl	external	bridging	2.622 ± 0.014	2.580 ± 0.034
	external	external	2.732 ± 0.039	2.674 ± 0.057
	bridging	external	2.873 ± 0.015	2.876 ± 0.151
Sb−I	external	bridging	2.936 ± 0.015	2.871 ± 0.010
	external	external	3.031 ± 0.037	3.012 ± 0.000
	bridging	external	3.098 ± 0.007	3.216 ± 0.036
Sb−Br	external	bridging	2.717 ± 0.000	2.631 ± 0.008
	external	external	2.821 ± 0.036	2.810 ± 0.016
	bridging	external	2.950 ± 0.011	3.050 ± 0.036
Sb−Cl	external	bridging	2.520 ± 0.038	2.426 ± 0.032
	external	external	2.676 ± 0.045	2.681 ± 0.053
	bridging	external	2.915 ± 0.067	2.962 ± 0.051

in the Supporting Information present the experimental and calculated vibrational frequency and intensity data for MX_6^{3-} anions for M = Bi and for X = I, Br, and Cl, while Tables S4−S6 do this for M = Sb. Tables S7−S9 report the results for $Bi_2X_9^{3-}$ anions, and Tables S10−S12 do this for $Sb_2X_9^{3-}$ anions. Finally, Tables S13−S19 present the data for the $M_2X_{10}^{4-}$ and MX_5^{2-} species for M = Bi and Sb. We summarize the results in Table 4, where the range of calculated and observed frequencies for the υ_{EE}, υ_{EB}, and υ_B M−X stretching modes are given for M = Bi and Sb and where X = I, Br, and Cl. Each anion has several vibrations of one type which span a broad frequency range and have different symmetry species. Thus, the frequency ranges can be seen to be large. However, it is clear from both the calculated and observed data that each bismuthate and each antimonite anion has $\upsilon_{EB} > \upsilon_{EE} > \upsilon_B$ as expected from the *trans* effect. In Table 4, to assist in further recognizing this trend, we also present specific calculated and observed frequencies for the symmetric υ_{EB}, υ_{EE}, and υ_B vibrations of the $M_2X_{10}^{4-}$ anions.

We will now make some observations about the specific data in the Supporting Information tables. It should again be emphasized that the computations are for independent free-standing anions and the experimental vibration spectra are those from species where the cation has a significant effect. For example, the A_{1g}, E_g, and T_{1u} Bi−I stretching frequencies for BiI_6^{3-} are 119, 105, and 110 cm^{-1}, respectively, when the cation is n-$C_3H_7NH_3^+$ but increase to 139, 128, and 135 cm^{-1} when the cation is $Cr(en)_3^{3+}$. The computed values are 104, 85, and 106 cm^{-1}, respectively, and agree much better with the n-$C_3H_7NH_3^{1+}$ system. As is evident in Table 4 and in the data in the Supporting Information tables, the calculated frequencies for the gas-phase anions tend to be about 10% lower than the experimental values. However, the effect of replacing one cation by another can affect the frequencies considerably more than that.

The Supporting Information tables also present the calculated PEDs for each M−X stretching vibration for each anion. These confirm that the highest frequencies are mostly υ_{EB} with smaller contributions from the υ_{EE} and υ_B stretchings. All of the bending modes together typically contribute less than 30%. The next highest group of frequencies are those for the υ_{EE} modes. These again have smaller contributions from the other two types of stretching modes and the bending modes. The υ_B stretching modes are the most coupled to the bending modes as they are the lowest in frequency and not much separated from the bending modes.

In addition to the primary observations described above, there are a few unusual features found from the vibrational calculations, and these can be seen by a more detailed inspection of the Supporting Information. For example, for $Sb_2Cl_{10}^{4-}$ there is a very strong coupling between the A_g υ_{EB} stretching and an A_g bending motion giving rise to vibrational frequencies of 258 and 211 cm^{-1}. This makes it seem at first

dx.doi.org/10.1021/ic302082a | Inorg. Chem. 2013, 52, 4244−4249

Table 4. Observed and Calculated Vibrational Frequencies for M−X Stretching Modes

			frequency range (cm^{-1})			
			calcd		obsd	
M−X	type	*trans*-halogen	range	sym stretch[a]	range	sym stretch[a]
Bi−I	external	bridging	112−136	126	110−138	N/A
	external	external	85−107	107	105−139	N/A
	bridging	external	75−113	99	80−99	N/A
Bi−Br	external	bridging	149−177	171	156−198	169
	external	external	115−148	143	123−164	142
	bridging	external	88−145	131	99−150	106
Bi−Cl	external	bridging	226−272	272	238−294	279
	external	external	164−227	222	169−255	244
	bridging	external	113−200	161	129−246	157
Sb−I	external	bridging	117−160	140	134−181	154
	external	external	84−127	110	100−135	100
	bridging	external	78−114	99	85−129	[95][b]
Sb−Br	external	bridging	157−196	188	164−215	205
	external	external	109−161	144	129−178	147
	bridging	external	84−146	126	110−155	[130][b]
Sb−Cl	external	bridging	229−316	316	279−323[c]	N/A
	external	external	164−256	211	174−282	N/A
	bridging	external	77−192	178	N/A	N/A

[a]Symmetric stretching for $M_2X_{10}^{2-}$ species. [b]Estimated. [c]The lowest expected frequency near 230 cm^{-1} was not observed.

glance that there is an extra stretching vibration. Other couplings in the other metalates can also be noticed.

The most important feature to reiterate about the vibrational calculations and observed spectra is that the *trans* effect is well supported by the data in Table 4 and the Supporting Information tables. The M−X stretching frequencies for external M−X bonds across from bridging bonds tend to be about 20% higher than those across from other external bonds. This is true for the bismuthates and antimonates and for X = I, Br, and Cl.

CONCLUSIONS

In our original work[1,23] postulating the *trans* effect, our conclusions were based on the fact that higher vibrational frequencies were observed for the M−X stretching modes for bonds across from bridging atoms. At that time there were only limited crystal structure data, but what there were also supported the concept of the *trans* effect. Over the past 30 years much more crystallographic data has now become available so it has become even more meaningful to carry out these theoretical calculations which can be compared to experimental results.

Even while all of the experimental structural and vibrational studies of the halobismuthates and antimonates clearly support the "*trans* effect," it can be argued that the computational results presented here do the best job of providing the expected bond distances and vibrational frequencies for noninteracting anions. This is the case since the calculations totally ignore any perturbations that are caused by the cations present. Examination of the experimental data clearly shows that the choice of cation can have a significant effect on which structure results, on what the bond distances are, and on what the vibrational frequencies are.

ASSOCIATED CONTENT

Supporting Information

Listings of experimental and calculated vibrational frequencies for the stretching vibrations of various halobismuthates and haloantimonates. This material is available free of charge via the Internet at http://pubs.acs.org.

AUTHOR INFORMATION

Corresponding Author

*E-mail: laane@mail.chem.tamu.edu.

Notes

The authors declare no competing financial interest.

ACKNOWLEDGMENTS

We thank the Robert A. Welch Foundation (Grant A-0396) for financial support. Computations were carried out on the Texas A&M Department of Chemistry Medusa computer system funded by the National Science Foundation, Grant CHE-0541587. The original halobismuthates and haloantimonates were first prepared by Professor Roger Whealy of Texas A&M University, and the crystal structures were determined by Edward A. Meyers of Texas A&M.

REFERENCES

(1) Laane, J.; Jagodzinski, P. W. *Inorg. Chem.* **1980**, *19*, 44.
(2) Bi, W.; Louvain, N.; Mercier, N.; Lucb, J.; Sahraoui, B. *CrystEngComm* **2007**, *9*, 298.
(3) Lindsjö, M.; Fischer, A.; Kloo, L. *Z. Anorg. Allg. Chem.* **2005**, *631*, 1497.
(4) Samet, A.; Ahmed, A.; Mlayah, A.; Boughzala, H.; Hlil, E.; Abid, Y. *J. Mol. Struct.* **2010**, *977*, 72.
(5) Lazarini, F. *Acta Crystallogr., Sect. B: Struct. Sci.* **1978**, *34*, 2288.
(6) Lazarini, F. *Acta Crystallogr., Sect. B: Struct. Sci.* **1980**, *36*, 2748.
(7) McPherson, W. G.; Meyers, E. A. *J. Phys. Chem.* **1968**, *72*, 3117.
(8) Work, R.; Good, M. *Spectrochim. Acta, Part A* **1973**, *29*, 1547.
(9) Chabot, B.; Parthi, E. *Acta Crystallogr., Sect. B: Struct. Sci.* **1978**, *34*, 645.
(10) Lazarini, F. *Acta Crystallogr., Sect. C: Cryst. Struct. Commun.* **1987**, *C43*, 875.
(11) Goforth, A. M.; Peterson, L.; Smith, M. D.; Loye, H. C. *J. Solid State Chem.* **2005**, *178*, 3529.
(12) Wojtaś, M.; Jakubas, R.; Ciunik, Z.; Medycki, W. *J. Solid State Chem.* **2004**, *177*, 1575.
(13) Lazarini, F. *Acta Crystallogr., Sect. B: Struct. Sci.* **1977**, *33*, 2686.
(14) Lazarini, F. *Acta Crystallogr., Sect. B: Struct. Sci.* **1977**, *33*, 2961.

(15) Hrizi, C.; Samet, A.; Abid, Y.; Chaabouni, S.; Fliyou, M.; Koumina, A. *J. Mol. Struct.* **2011**, *992*, 96.
(16) Bi, W.; Louvain, N.; Mercier, N.; Luc, J.; Rau, I.; Kajzar, F.; Sahraoui, B. *Adv. Mater.* **2008**, *20*, 1013.
(17) Lazarini, F.; Leban, I. *Acta Crystallogr., Sect. B: Struct. Sci.* **1980**, *36*, 2745.
(18) Lazarini, F. *Acta Crystallogr., Sect. B: Struct. Sci.* **1980**, *36*, 2748.
(19) Piecha, A.; Kinzhybalo, V.; Jakubas, R.; Baran, J.; Medycki, W. *Solid State Sci.* **2007**, *9*, 1036.
(20) McPherson, W.; Meyers, E. *J. Phys. Chem.* **1968**, *72*, 532.
(21) Geiser, U.; Wang, H. H.; Budz, S. M.; Lowry, M. J.; Williams, J. M.; Ren, J.; Whangbo, M. *Inorg. Chem.* **1990**, *29*, 1611.
(22) Robertson, B. K.; McPherson, W. G.; Meyers, E. H. *J. Phys. Chem.* **1967**, *71*, 3531.
(23) Laane, J.; Jagodzinski, P. W. *J. Raman Spectrosc.* **1980**, *9*, 22.
(24) Piecha, A.; Gągor, A.; Pietraszko, A.; Jakubas, R. *J. Solid State Chem.* **2010**, *183*, 3058.
(25) Płowaś, I.; Białońska, A.; Jakubas, R.; Bator, G.; Zarychta, B.; Baran, J. *Chem. Phys.* **2010**, *375*, 16.
(26) Carmalt, C.; Farrugia, L.; Norman, N. *Z. Anorg. Allg. Chem.* **1995**, *621*, 47.
(27) Chabot, B.; Parthi, E. *Acta Crystallogr., Sect. B: Struct. Sci.* **1978**, *B34*, 645.
(28) Ho, D.; Riley, W. C.; Jacobson, R. A. *Cryst. Struct. Commun.* **1978**, *7*, 111.
(29) Bujak, M.; Zaleski, J. *Acta Crystallogr., Sect. E: Struct. Rep. Online* **2007**, *63*, m102.
(30) Hubbard, C.; Jacobson, R. *Inorg. Chem.* **1972**, *11*, 2247.
(31) Louvain, N.; Mercier; Boucher, F. *Inorg. Chem.* **2009**, *48*, 879.
(32) Bukvetskii, V.; Sedakova, T. V.; Mirochnik, A. G. *J. Struct. Chem.* **2009**, *50*, 322.
(33) Kulicka, B.; Jakubas, R.; Bator, G.; Ciunik, Z.; Medycki, W. *J. Phys.: Condens. Matter* **2004**, *16*, 8155.
(34) Jarraya, S.; Salah, A.; Daoud, A. *Acta Crystallogr., Sect. C: Cryst. Struct. Commun.* **1993**, *49*, 1594.
(35) Lazarini, F. *Acta Crystallogr., Sect. C: Cryst. Struct. Commun.* **1987**, *43*, 637.
(36) Herdtweck, E.; Kreusel, U. *Acta Crystallogr., Sect. C: Cryst. Struct. Commun.* **1993**, *49*, 318.
(37) Benetollo, F.; Bombieri, G.; Alonzo, G.; Bertazzi, N.; Casella, G. *J. Chem. Crystallogr.* **1998**, *28*, 791.
(38) Wang, Y.; Xu, L. *J. Mol. Struct.* **2008**, *875*, 570.
(39) Yang, Z.; Chen, G.; Xua, W.; Fan, Z. *Acta Crystallogr., Sect. E: Struct. Rep. Online* **2009**, *E65*, m887.
(40) Battaglia, L.; Corradi, A. *Inorg. Chim. Acta* **1986**, *121*, 131.
(41) Benetollo, F.; Bombieri, G.; Del Pra, A.; Alonzo, G.; Bertazzi, N. *Inorg. Chim. Acta* **2001**, *319*, 49.
(42) Morss, L.; Robinson, W. *Acta Crystallogr., Sect. B: Struct. Sci.* **1972**, *B28*, 653.
(43) Ouasri, A.; Jeghnou, H.; Rhandour, A.; Dhamelincourt, M.; Dhamelincourt, P.; Mazzah, A.; Roussel, P. *J. Raman Spectrosc.* **2005**, *36*, 791.
(44) Rao, A. S.; Babu, E. S.; Swamy, K. C. K.; Das, S. K. *Polyhedron* **2010**, *29*, 1706.
(45) Gerasimenko, A.; Karaseva, E.; Polishchuk, A. *Acta Crystallogr., Sect. E: Struct. Rep Online* **2008**, *E64*, m378.
(46) Khelifi, M.; Zouari, R.; Salah, A. *Acta Crystallogr., Sect. E: Struct. Rep. Online* **2008**, *E64*, i80.
(47) Bigoli, F.; Lanfranchi, M.; Pellinghelli, M. *Inorg. Chim. Acta* **1984**, *90*, 215.
(48) Rhandour, A.; Ouasri, A.; Roussel, P.; Mazzah, A. *J. Mol. Struct.* **2011**, *990*, 95.
(49) Chaabouni, S.; Kamoun, S.; Jaud, J. *J. Chem. Crystallogr.* **1998**, *28*, 209.
(50) Ferjani, H.; Boughzala, H.; Driss, A. *Acta Crystallogr.* **2012**, *E68*, m615.
(51) Wang, Y. C. *Acta Crystallogr.* **2012**, *E68*, m181.
(52) Vezzosi, I. *Inorg. Chim. Acta* **1984**, *89*, 151.
(53) Bujak, M.; Osadczuk, P.; Zaleski, J. *Acta Crystallogr., Sect. C: Cryst. Struct. Commun.* **2001**, *C57*, 388.
(54) Schroeder, D.; Jacobson, R. *Inorg. Chem.* **1973**, *12*, 210.
(55) Wojtaś, M.; Jakubas, R. *J. Phys.: Condens. Matter* **2004**, *16*, 7521.
(56) Zarychta, B.; Bujak, M.; Zaleski, J. *Z. Naturforsch., B: Chem. Sci.* **2007**, *62*, 44.
(57) Gerasimenko, A. V.; Polishchuk, A. V.; Karaseva, E. T.; Karasev, V. E. *Russ. J. Coord. Chem.* **2008**, *34*, 647.
(58) Wojtaś, M.; Jakubas, R.; Baran, J. *Vib. Spectrosc.* **2005**, *39*, 23.
(59) Wojtaś, M.; Bator, G.; Baran, J. *Vib. Spectrosc.* **2003**, *33*, 143.
(60) Benedetti, A.; Fabretti, A.; Malavasi, W. *J. Crystallogr. Spectrosc. Res.* **1992**, *22*, 145.
(61) Piecha, A.; Kinzhybalo, V.; Jakubas, R.; Baran, J.; Medycki, W. *Solid State Sci.* **2007**, *9*, 1036.
(62) Bowmaker, G.; Junk, P.; Lee, A. M.; Skelton, B. W.; White, A. H. *Aust. J. Chem.* **1998**, *51*, 293.
(63) Khili, H.; Chaari, N.; Fliyou, M.; Koumina, A.; Chaabouni, S. *Polyhedron* **2012**, *36*, 30.
(64) Zouari, F.; Salah, A. *Phase Transitions* **2005**, *78*, 317.
(65) Tarasiewicz, J.; Jakubas, R.; Bator, G.; Zaleski, J.; Baran, J.; Medycki, W. *J. Mol. Struct.* **2009**, *932*, 6.
(66) Allen, G.; McMeeking, R. *Inorg. Chim. Acta* **1977**, *23*, 185.
(67) Bator, G.; Jakubas, R.; Majerz, I.; Malarski, Z. *J. Mol. Struct.* **1992**, *274*, 1.
(68) Laitinen, R.; Steudel, R. *J. Chem. Soc., Dalton Trans.* **1986**, *1*, 1095.
(69) Varma, V.; Bhattacharjee, R.; Vasan, H.; Raot, C. *Spectrochim. Acta* **1992**, *48A*, 1631.
(70) Frisch, M. J.; Trucks, G. W.; Schlegel, H. B.; Scuseria, G. E.; Robb, M. A.; Cheeseman, J. R.; Scalmani, G.; Barone, V.; Mennucci, B.; Petersson, G. A.; Nakatsuji, H.; Caricato, M.; Li, X.; Hratchian, H. P.; Izmaylov, A. F.; Bloino, J.; Zheng, G.; Sonnenberg, J. L.; Hada, M.; Ehara, M.; Toyota, K.; Fukuda, R.; Hasegawa, J.; Ishida, M.; Nakajima, T.; Honda, Y.; Kitao, O.; Nakai, H.; Vreven, T.; Montgomery, Jr., J. A.; Peralta, J. E.; Ogliaro, F.; Bearpark, M.; Heyd, J. J.; Brothers, E.; Kudin, K. N.; Staroverov, V. N.; Kobayashi, R.; Normand, J.; Raghavachari, K.; Rendell, A.; Burant, J. C.; Iyengar, S. S.; Tomasi, J.; Cossi, M.; Rega, N.; Millam, J. M.; Klene, M.; Knox, J. E.; Cross, J. B.; Bakken, V.; Adamo, C.; Jaramillo, J.; Gomperts, R.; Stratmann, R. E.; Yazyev, O.; Austin, A. J.; Cammi, R.; Pomelli, C.; Ochterski, J. W.; Martin, R. L.; Morokuma, K.; Zakrzewski, V. G.; Voth, G. A.; Salvador, P.; Dannenberg, J. J.; Dapprich, S.; Daniels, A. D.; Farkas, Ö.; Foresman, J. B.; Ortiz, J. V.; Cioslowski, J.; Fox, D. J. *Gaussian 09*, revision B.01; Gaussian, Inc.: Wallingford, CT, 2009.
(71) Rishard, M.; Irwin, M.; Laane, J. *J. Phys. Chem. A* **2007**, *111*, 825.
(72) Boopalachandran, P.; Laane, J. *Spectrochim. Acta, Part A* **2011**, *79*, 1191.
(73) Ocola, J.; Bauman, E.; Laane, J. *J. Phys. Chem. A* **2011**, *115*, 6531.
(74) Al-Saadi, A.; Laane, J. *Spectrochim. Acta, Part A* **2008**, *71A*, 326.
(75) Al-Saadi, A.; Laane, J. *Organometallics* **2008**, *27*, 3435.
(76) Al-Badri, N. I.; Al-Jallal, N. A.; El-Azhary, A. A. *Theor. Chem. Acc.* **2011**, *130*, 919.
(77) Strenalyuk, T.; Samdal, S.; Vidar Volden, H. *J. Phys. Chem. A* **2008**, *112*, 9075.
(78) Nhat, P. V.; Nguyen, M. T. *Phys. Chem. Chem. Phys.* **2011**, *13*, 16254.
(79) Lagutschenkov, A.; Sinha, R. K.; Maitre, P.; Dopfer, O. *J. Phys. Chem. A* **2010**, *114*, 11053.
(80) Choinopoulos, I.; Papageorgiou, I.; Coco, S.; Simandiras, E.; Koinis, S. *Polyhedron* **2012**, *45*, 255.
(81) Nhat, P.; Tai, T.; Nguyen, M. *J. Chem. Phys.* **2012**, *137*, 164312.